Nonlinear features of a micromaser in the semiclassical limit

Juan C. Retamal, Carlos Saavedra, and Edmundo Lazo
Departamento de Física, Facultad de Ciencias, Universidad de Tarapacá, Casilla 7-D, Arica, Chile
(Received 1 February 1993)

We study the chaotic behavior of the internal field in a micromaser with injected atomic coherence. The quantum dynamics provides a return map in the semiclassical limit which we study as a function of the reduced atom-field interaction time. Bifurcations, chaos, and transitions between bifurcation sequences appear in a broad range of the parameter space.

PACS number(s): 42.52.+x, 42.50.Lc

The micromaser remains as a system of central interest in quantum optics. Until now, nonclassical aspects of the interaction of an atom with a quantized field have been experimentally realized, namely, the collapses and revivals [1] and sub-Poissonian photon statistics [2]. The possibility of generated number states [3,4] and macroscopic superpositions of the electromagnetic field [5] has created a renewed interest in the micromaser research. Additional studies show that such states could be generated in different micromaser systems [6,7]. Recently, a discussion about the experimental feasibility of such predictions has been considered, including the cavity dissipation and the finite atomic lifetime effect [8,9]. A point of view which has not received much attention is related to the semiclassical limit of the micromaser theory. A preliminary analysis of such a limit has been considered for a micromaser pumped by atoms injected in the upper level, showing the existence of chaotic features in the internal field intensity [10]. A general formulation and characterization of such a limit is still open.

The aim of the present work is to consider the semiclassical dynamics of the internal field of a micromaser driven by coherently prepared two-level atoms. We consider the quantum theory of the micromaser in the Schrödinger picture and set the equations to the semiclassical limit, obtaining a return map for the field intensity. The return map is highly nonlinear with a rich parameter space which allows us to investigate a variety of regimes in which bifurcations and chaos could appear. The structure of our map resembles that of a circle map [11], but contains an enhanced parameter space. The complete characterization of the nonlinear dynamics in the semiclassical limit opens new possibilities in the micromaser study.

It is well known that the internal dynamics of a micromaser is driven by two processes, the gain represented by the atom-field interaction during a flight time τ and the dissipation introduced through the interaction of the field with a thermal bath. The coarse-grained derivation of the master equation for a micromaser considers the superposition of both effects. This approximation assumes that gain and dissipation act independently in the dynamics. This last statement is only valid when characteristic times associated with the injection and dissipation processes satisfy $\gamma^{-1} \gg r^{-1}$, where γ is the loss rate and r is the atomic injection rate. In a discrete time scale it is not possible to write an exact equation that includes at the same time both the gain and the dissipation. We know that the atoms enter with a delay time between them given by the inverse of the pump rate, $r^{-1}=t_p+\tau$, where t_p is the time for which the cavity does not have atoms. In order to overcome the problem of simultaneous treatment of gain and loss, the physical situation in which $t_p \gg \tau$ is considered, so that gain and dissipation can be assumed to be affecting the field dynamics independently. This last assumption allows us to write the following map for the density matrix of the field:

$$\rho^{(k+1)}=e^{Lt_p}\mathcal{M}\rho^{(k)} . \tag{1}$$

The operators $\mathcal{M}$ and L represent the gain and the cavity losses, respectively. The gain operator is given by

$$\mathcal{M}\rho^{(k)}=\mathrm{tr}_{\mathrm{atom}}U(\tau)\rho_{(\mathrm{atom})}\otimes\rho^{(k)}U^{\dagger}(\tau) , \tag{2}$$

where $U(\tau)$ is the evolution operator for the Jaynes-Cummings model [12]. The loss operator at zero temperature is given by

$$L\rho(t)=\frac{\gamma}{2}(2a\rho a^{\dagger}-a^{\dagger}a\rho-\rho a^{\dagger}a) , \tag{3}$$

where γ denotes the cavity decay rate for the field. Equation (1) implicitly assumes a regular atomic injection into the cavity. The problem of an arbitrary injection statistics has been considered in the framework of a continuous time scale within the coarse-grained approximation [13]. In the context of Eq. (1) the real problem of a particular atomic injection process can be attacked considering a simulation of this process, introducing a suitable choice of the injection time intervals. In the present work we consider just regular injection.

Turning back to Eq. (2) the quantity $\rho_{(\mathrm{atom})}\otimes\rho^{(k)}$ represents the initial condition for the atom-field system after k atoms passed through the cavity. Considering atoms injected in a coherent superposition of the atomic levels, Eq. (1) reads

$$\begin{aligned}\rho^{(k+1)}=e^{t_pL}\{&\rho_{aa}(\mathcal{C}\rho^{(k)}\mathcal{C}+\mathcal{S}^{\dagger}\rho^{(k)}\mathcal{S})\\&+\rho_{bb}(\overline{\mathcal{C}}\rho^{(k)}\overline{\mathcal{C}}+\mathcal{S}\rho^{(k)}\mathcal{S}^{\dagger})\\&+i\rho_{ab}(\mathcal{C}\rho^{(k)}\mathcal{S}^{\dagger}-\mathcal{S}^{\dagger}\rho^{(k)}\overline{\mathcal{C}})\\&+i\rho_{ba}(\overline{\mathcal{C}}\rho^{(k)}\mathcal{S}-\mathcal{S}\rho^{(k)}\mathcal{C})\} ,\end{aligned} \tag{4}$$

with

$$\mathcal{C}=\cos(\phi\sqrt{aa^\dagger}),\quad \overline{\mathcal{C}}=\cos(\phi\sqrt{a^\dagger a}\,)\ ,$$
$$\mathcal{S}=\frac{\sin(\phi\sqrt{aa^\dagger})}{\sqrt{aa^\dagger}}a\ , \tag{5}$$

where $\phi=g\tau$ plays the role of an adimensional time and g is the coupling constant between atoms and the field. The previous expression allows us to calculate the discrete dynamics of the average photon number by tracing the operator $\hat{n}=a^\dagger a$ with respect to $\rho^{(k+1)}$. By using the cyclic property of the trace it is not difficult to show that

$$\langle\hat{n}\rangle^{(k+1)}=e^{-\gamma t_p}\sum_{n=0}^{\infty} n\,(\mathcal{M}\rho^{(k)})_{nn}\ , \tag{6}$$

where the sum in this expression explicitly reads

$$\sum_{n=0}^{\infty} n\,(\mathcal{M}\rho^{(k)})_{nn}=\langle\hat{n}\rangle^{(k)}+\rho_{aa}\langle\sin^2(\phi\sqrt{\hat{n}+1})\rangle^{(k)}-\rho_{bb}\langle\sin^2(\phi\sqrt{\hat{n}}\,)\rangle^{(k)}$$
$$+2|\rho_{ab}|\sin(\theta_{ab}-\theta)\sum_{n=0}^{\infty}\cos(\phi\sqrt{n+1})\sin(\phi\sqrt{n+1})|\rho^{(k)}_{nn+1}|\ . \tag{7}$$

We observe that the phase of the atomic coherence θ_{ab} couples with the phase of the first off-diagonal density matrix elements, $|\rho_{nn+1}|e^{i\theta}$. In our analysis we eliminate the phase dependence, assuming a phase-locking condition $\theta_{ab}-\theta=\pi/2$. This assumption is in agreement with a Fokker-Planck equation analysis, where a similar equation arises. With this simplification Eq. (6) represents a quantum map for the field intensity in terms of the number of atoms crossing the cavity. One of the interesting possibilities of this equation is realized in the semiclassical limit, in which photon statistics is sharply peaked around a certain value of the photon intensity [14]. In that situation we can assume that quantum fluctuations go to zero in such a way that quantum variables can be considered as c-number variables. Let us consider the average photon number $\langle\hat{n}\rangle^{(k)}$, after k atoms have passed through the cavity, in the semiclassical limit. Let us denote it in this limit by the c-number variable ψ_k, so that Eq. (6) in the semiclassical limit reads

$$\psi_{k+1}=e^{-\gamma t_p}[\psi_k+A\sin^2(\phi\sqrt{\psi_k})+B\sin(2\phi\sqrt{\psi_k})]\ , \tag{8}$$

where $A=\rho_{aa}-\rho_{bb}$ is the difference of initial populations and B is the initial coherence ρ_{ab}. For a pure atomic state $B=B_{\max}=\sqrt{(1-A^2)}/2$. Equation (8) represents a map for the internal electromagnetic field of the micromaser kicked by a stream of two-level atoms. This map is completely general because it depends on four physical parameters, namely, the factor $\alpha=e^{-\gamma t_p}$, which is related to the number of atoms which enter the cavity during the time in which the field decays, the reduced atom-field interaction time ϕ, and the initial atomic coherence parameters A and B which are only dependent for a pure atomic state. The injected atomic coherence plays an important role in increasing the nonlinearity of the return map. We have to point out that in the particular case $B=0$ this map reduces to the map obtained in Ref. [3]. On the other hand, in the particular case of an initially pure atomic state, that is, $B=B_{\max}$, it can be reduced to a map similar to the circle map. The main difference between this map and the circle map is the presence of the parameter α as a multiplicative parameter and the parameter ϕ inside the trigonometric function which are very important for the nonlinear behavior.

The high nonlinearity of the map given in Eq. (8) opens new possibilities to study the existence of bifurcations and chaos in different regimes. Here we are mainly interested in analyzing the dissipative case, $\alpha<1$, which is physically more realistic. However, a rich nonlinear structure also appears in the nondissipative regime [15].

A first step in the analysis of the return map is to characterize the fixed-point structure. We are tempted to consider in the first place the nondissipative regime with $\alpha=e^{-\gamma t_p}=1$. In this case it is straightforward to show that the fixed points of $\psi_{k+1}=f(\psi_k)$ defined by Eq. (8) are given by

$$\psi_q^*=q^2\pi^2\phi^{-2},\quad q=0,1,2,\ldots,\ \text{unstable}\ , \tag{9}$$
$$\psi_p^*=\left[p\pi-\arctan\left[\frac{2B}{A}\right]\right]^2\phi^{-2}\ ,$$
$$p=0,1,2,\ldots,\ \text{stable}\ . \tag{10}$$

Stability of fixed points is given by the condition $|f'(\psi)|<1$ and there are stable and unstable solutions. This is illustrated in Fig. 1, where the return map is plotted for $\alpha=1$, $A=0.5$, $B=0.433$, and $\phi=3.03$. We observe that between two unstable fixed points there is a stable fixed point of the map. The position of the unstable fixed points depends only on the reduced time ϕ. In

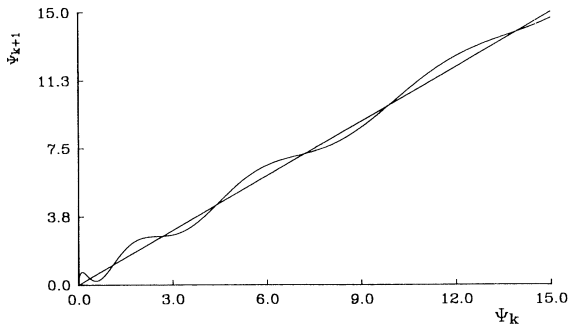

FIG. 1. Return map for $\alpha=1.0$, $A=0.5$, $B=0.433$, $\phi=3.03$.

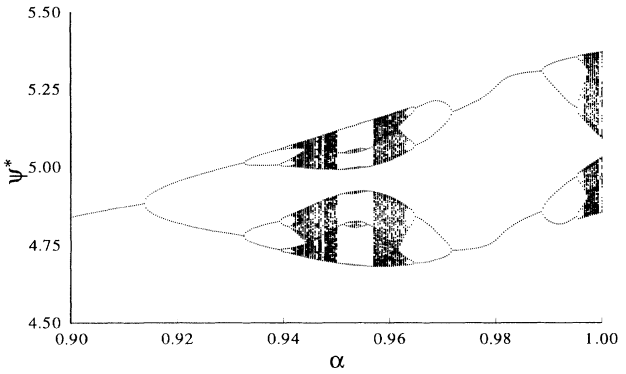

FIG. 2. Bifurcation diagram in terms of α for $A=0.2$, $B=B_{\max}$, $\phi=13.37$ with the initial condition $\psi_0=4.8$.

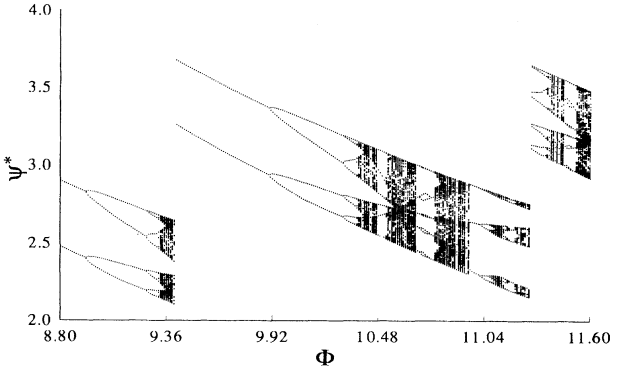

FIG. 4. Bifurcation diagram for $A=0.2$, $B=B_{\max}$, $\alpha=0.99$, and the initial condition $\psi_0=2.8$.

addition, the stable fixed points depend on the values of A and B. The fixed-point structure changes when B goes to zero because the stable fixed points converge to the upper unstable ones, giving rise to the marginally stable fixed points analyzed by Filipowicz, Javanainen, and Meystre [3]. The interval between two neighboring unstable fixed points defines a basin of attraction. All the points in this region give rise to the same attractor. When B goes to zero the situation changes drastically, because near initial points between two marginally stable fixed points belong to different basins of attraction, so that starting from different initial points in this region gives rise to different attractors. If we compare these semiclassical features with the quantum counterpart of the model, the situation with $B\neq 0$ resembles the dynamics of the system in disconnected blocks of the Fock space [5], because an initial condition within a given basin of attraction evolves to a steady state contained in the same basin of attraction and a typical trapped dynamics takes place. The case $B=0$ is not reminiscent of this trapped dynamics.

In the dissipative regime of the system the fixed-point structure exhibits radical differences. We notice that dissipation, introduced through the exponential in Eq. (8) ($\alpha<1$), produces a shift in the slope of the sinusoidal curve with respect to the diagonal $\psi_{k+1}=\psi_k$. The curve begins to separate from the diagonal, producing a finite string of fixed points, conversely to the nondissipative case in which the fixed-point set is infinite. In this case, it is a nontrivial problem to characterize the fixed points, so we proceed to iterate the map to obtain the fixed points as a function of the parameters A, B, and ϕ. A preliminary analysis of the fixed points and chaotic behavior of the field, considering $\alpha=e^{-\gamma\tau}$ as a control parameter and initial coherence equal to zero ($B=0$), was carried out by Filipowicz, Javanainen, and Meystre [3]. In this case the existence of chaos is natural to the structure of the return map when α is the control parameter. As we can see in Eq. (8), there is a close analogy with the structure of a logistic map, that is, a nonlinear function with a multiplicative parameter. More explicitly, considering the first two terms in a series expansion of the sinusoidal function, it gives rise to a logistic-type map. This last statement occurs independently whether or not the atom is injected in a coherent superposition. An example of such features is shown in Fig. 2 (see also Fig. 3), where the fixed-point structure is plotted as a function of α for $A=0.2$, $B=B_{\max}$, $\phi=13.37$ for an initial condition $\psi_0=4.8$.

The return map offers additional possibilities to search chaotic behavior, namely, the injected atomic coherence and the reduced interaction time ϕ. In this work we are concerned with the reduced atom-field interaction time. As it is induced from the semiclassical map, the main effect of the variation of ϕ is to increase the frequency of the sinusoidal curve on the diagonal. As a consequence, for a given initial condition ψ_0 of the field, the continuous variation of ϕ causes ψ_0 to belong to different basins of attraction. This effect explains the successive transitions which experience the field intensity for different values of ϕ, as is observed in Fig. 4. In this calculation we considered atoms in a coherent superposition with $B=B_{\max}$, for difference of populations $A=0.2$ and dissipation

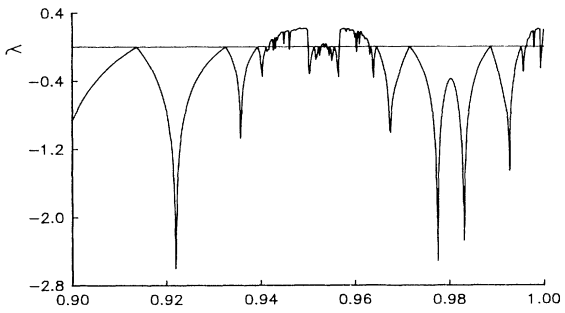

FIG. 3. Lyapunov's exponent of Fig. 2.

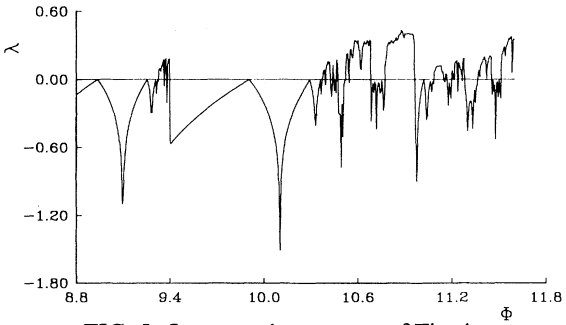

FIG. 5. Lyapunov's exponent of Fig. 4.

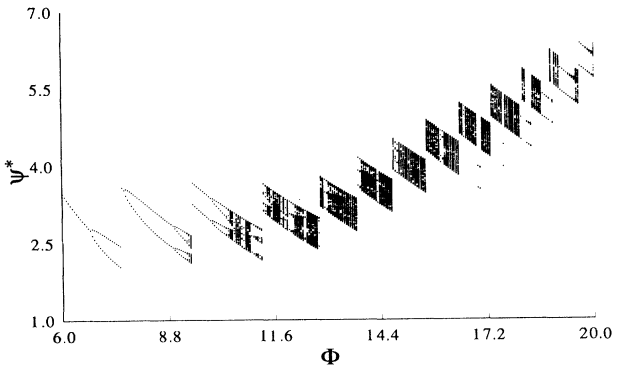

FIG. 6. Bifurcation diagram for the same parameters as in Fig. 4, in an extended region of ϕ.

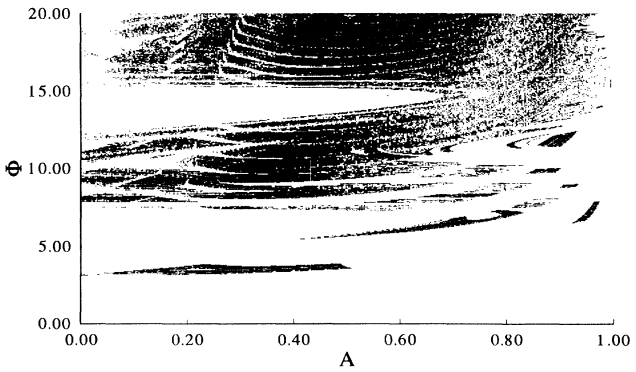

FIG. 7. Phase diagram of chaotic regions in the plane $\{A,\phi\}$.

$\alpha=0.99$, using an initial point $\psi_0=2.8$. The appearance of bifurcations and tendency to chaos for different values of ϕ is clearly observed. In Fig. 5 the Lyapunov exponent corresponding to Fig. 4 shows the existence of chaos ($\lambda>0$) in this case. The same situation is considered in Fig. 6 in an extended range of ϕ. We observe that increasing the value of ϕ the field experiences transitions to higher intensities. This behavior is explained because the field attractors in the intensity axis increase when ϕ is increased.

A more complete search of chaotic behavior is the parameter space $\{A,\phi\}$ has been considered when $B=B_{\max}(A)$ for a fixed dissipation $\alpha=0.99$ and an initial point $\psi_0=2.8$. In Fig. 7 we show the chaotic zones (black points) in the space $\{A,\phi\}$ where the Lyapunov exponent is positive. This diagram allows us to visualize the behavior of the field intensity for a fixed difference of initial population A as a function of the reduced time ϕ. The case shown in Figs. 4 and 5 corresponds to a single vertical line of this general map. Simultaneously we can observe that there exist a similar structure of bifurcations and chaos for a fixed reduced time ϕ and varying initial population A. The existence of chaotic behavior in terms of A as a control parameter is comparable with that occurring in the circle map [11].

In the present work we have analyzed the nonlinear behavior of a micromaser in the semiclassical limit. We found that the system evolves to a chaotic regime in a broad range of the parameter space. The main result of this work is that the chaotic behavior is obtained in terms of the reduced interaction time ϕ as a control parameter. This gives an alternative physical picture which allows us to find chaos at higher values of the field intensity. This result is very important, because the semiclassical limit is well justified in a high-intensity regime of the system such that quantum fluctuations tend to vanish compared with the average intensity. On the other hand, it is important to point out that the transitions between different bifurcation sequences are an interesting aspect which require a deeper analysis. Problems such as the characterization of the different routes to chaos, the effect of additive noise, and the simulation of the measurement process are in progress now [16].

We are grateful to Pedro Orellana for his collaboration and to the Physics Faculty of Pontificia Universidad Católica de Chile where part of this work was done. We acknowledge FONDECYT and Universidad de Tarapacá for financial support.

[1] G. Rempe, H. Walther, and N. Klein, Phys. Rev. Lett. **58**, 353 (1987).
[2] D. Meschede, H. Walther, and G. Müller, Phys. Rev. Lett. **54**, 551 (1985).
[3] P. Filipowicz, J. Javanainen, and P. Meystre, J. Opt. Soc. Am. B **3**, xx (1986).
[4] J. Krause, M. O. Scully, and H. Walther, Phys. Rev. A **36**, 4567 (1987).
[5] J. J. Slosser, P. Meystre, and S. L. Braunstein, Phys. Rev. Lett. **63**, 934 (1989); J. J. Slosser and P. Meystre, Phys. Rev. A **41**, 3867 (1990).
[6] J. C. Retamal, L. Roa, and C. Saavedra, Phys. Rev. A **45**, 1876 (1992).
[7] M. Orszag, R. Ramirez, J. C. Retamal, and L. Roa, Phys. Rev. A **45**, 6717 (1992).
[8] L. Roa, J. C. Retamal, and C. Saavedra, Phys. Rev. A **47**, 620 (1993).
[9] Shi-Yao Zhu and L. Z. Wang, Phys. Rev. A **42**, 5798 (1990); Shi-Yao Zhu, L. Z. Wang, and Heidi Fearn, *ibid.* **44**, 737 (1991).
[10] P. Meystre and E. M. Wright, in *Chaos, Noise and Fractals,* edited by E. R. Pike and L. A. Lugiato, Malvern Physics Series (Hilger, London, 1987).
[11] R. V. Jensen and E. R. Jessup, J. Stat. Phys. **43**, 369 (1986).
[12] M. Sargent III, M. O. Scully, and W. E. Lamb, *Laser Physics* (Addison-Wesley, Reading, MA, 1974).
[13] J. Bergou, L. Davidovich, M. Orszag, C. Benkert, M. Hillery, and M. Scully, Opt. Commun. **72**, 82 (1989); Y. M. Golubev and I. V. Sokolov, Zh. Eksp. Teor. Fiz. **87**, 408 (1986) [Sov. Phys. JETP **60**, 234 (1984)].
[14] A sharply peaked distribution can be found too for nonclassical states, such as the case of sub-Poissonian fields. For a general description of nonclassical states, see, for example, R. Loudon and P. L. Night, J. Mod. Opt. **34**, 709 (1987). This case needs a different treatment from that presented here.
[15] E. Lazo, J. Retamal, and C. Saavedra (unpublished).
[16] C. Saavedra, E. Lazo, and J. Retamal (unpublished).